Double Perovskites

International Edition: DOI: 10.1002/anie.201603526
German Edition: DOI: 10.1002/ange.201603526

Double Double Cation Order in the High-Pressure Perovskites $MnRMnSbO_6$

*Elena Solana-Madruga, Ángel M. Arévalo-López, Antonio J. Dos Santos-García, Esteban Urones-Garrote, David Ávila-Brande, Regino Sáez-Puche, and J. Paul Attfield**

Abstract: *Cation ordering in ABO_3 perovskites adds to their chemical variety and can lead to properties such as ferrimagnetism and magnetoresistance in Sr_2FeMoO_6. Through high-pressure and high-temperature synthesis, a new type of "double double perovskite" structure has been discovered in the family $MnRMnSbO_6$ (R = La, Pr, Nd, Sm). This tetragonal structure has a 1:1 order of cations on both A and B sites, with A-site Mn^{2+} and R^{3+} cations ordered in columns and Mn^{2+} and Sb^{5+} having rock salt order on the B sites. The $MnRMnSbO_6$ double double perovskites are ferrimagnetic at low temperatures with additional spin-reorientation transitions. The ordering direction of ferrimagnetic Mn spins in $MnNdMnSbO_6$ changes from parallel to [001] below $T_C = 76$ K to perpendicular below the reorientation transition at 42 K at which Nd moments also order. Smaller rare earths lead to conventional monoclinic double perovskites (MnR)$MnSbO_6$ for Eu and Gd.*

ABO_3 perovskite oxides are a versatile class of materials with many notable physical and chemical properties. Further important variation arises from cation ordering within the basic structural arrangement. A 1:1 cation order in perovskites can occur in (100) layered, (110) columnar, or (111) rock salt arrangements, with cations ordered parallel to the cubic perovskite planes indicated. All three types have been observed for both A-cation-ordered $AA'B_2O_6$ and for B-ordered $A_2BB'O_6$ double perovskites,[1] amongst which layered $AA'B_2O_6$ and rock salt $A_2BB'O_6$ orders are the most common.[2] However $AA'BB'O_6$ "double double perovskites" with simultaneous 1:1 cation order at both A and B sites are much rarer, and only one of the nine possible combinations has previously been reported. This type combines the common (100) A-cation layered and (111) rock salt B-cation orders in several examples, such as $NaLaMgWO_6$ and $NaLaScNbO_6$.[3,4] We report herein a new double double perovskite type that has been discovered as part of an investigation of perovskites with Mn^{2+} ions at A sites.

A^{2+} cations in perovskites synthesized at ambient pressure are typically large, nonmagnetic atoms, such as A = Ca, Sr, Ba, Pb. However, materials with the smaller high-spin Mn^{2+} ion at A sites have been synthesized under high-pressure and high-temperature conditions. This may introduce additional magnetic functionality as found in $MnVO_3$ perovskite which is metallic due to itinerancy of the V^{4+} $3d^1$ states as in $CaVO_3$ and $SrVO_3$, but also has coexisting helimagnetic order of localized $S = 5/2$ Mn^{2+} spins.[5] Several $Mn_2BB'O_6$ double perovskites have also been synthesized at high pressures.[6,7] Mn_2FeSbO_6 has low-temperature incommensurate antiferromagnetic Mn spin order.[8] Mn_2FeReO_6 has a high Curie temperature of 520 K and similar ferrimagnetic and spin-polarized conducting properties to the much-studied magnetoresistive material Sr_2FeMoO_6, but also shows a novel switch from negative to large positive magnetoresistances at low temperatures driven by Mn^{2+} spin ordering.[9,10] In contrast, Mn_2MnReO_6 (Mn_3ReO_6) shows successive antiferromagnetic ordering transitions for Re and Mn spins at 99 and 109 K, respectively.[11] Our subsequent investigation of possible rare earth (R) double perovskites Mn_2RSbO_6, reported herein, has led to the discovery of a new double double perovskite type for $MnRMnSbO_6$ with large R cations, as well as more conventional (MnR)$MnSbO_6$ double perovskites formed for smaller rare earth metal ions.

$MnRMnSbO_6$ materials were synthesized at 10 GPa pressure and 1473 K in a Walker-type multianvil apparatus. Further experimental details are given in the Supporting Information. Small single crystals of $MnNdMnSbO_6$ were separated from the Pt capsule following a slow cooling experiment. Powder X-ray diffraction patterns (Figure 1 a, b) collected at the ALBA synchrotron showed that two different perovskite-related structures are formed, with large cations (R = La, Pr, Nd, or Sm) giving rise to one type of structure, whereas the smaller Eu and Gd centers lead to the formation of a different arrangement. The latter structure was identified as a conventional $A_2BB'O_6$ double perovskite with a typical monoclinic $P2_1/n$ distortion. Mn^{2+} and R^{3+} cations are disordered over the A sites while Mn^{2+} and Sb^{5+} have rock salt order over B and B′ sites.

The new double double $MnRMnSbO_6$ perovskite superstructure adopted by large R cations was solved through X-

[*] Dr. Á. M. Arévalo-López, Prof. J. P. Attfield
Centre for Science at Extreme Conditions (CSEC) and School of Chemistry, University of Edinburgh
Mayfield Road, Edinburgh EH9 3JZ (UK)
E-mail: j.p.attfield@ed.ac.uk
E. Solana-Madruga, Dr. D. Ávila-Brande, Prof. R. Sáez-Puche
Dpto. Quimica Inorganica I, Fac. Quimicas
Universidad Complutense de Madrid
28040 Madrid (Spain)
Dr. A. J. Dos Santos-García
Dpto. Ingeniería mecánica, química y diseño industrial, ETSIDI
Universidad Politécnica de Madrid
28012 Madrid (Spain)
Dr. E. Urones-Garrote
Centro Nacional de Microscopía Electrónica
Universidad Complutense de Madrid
28040 Madrid (Spain)

Supporting information for this article can be found under: http://dx.doi.org/10.1002/anie.201603526. Open data for this article are at: http://dx.doi.org/10.7488/ds/1408.

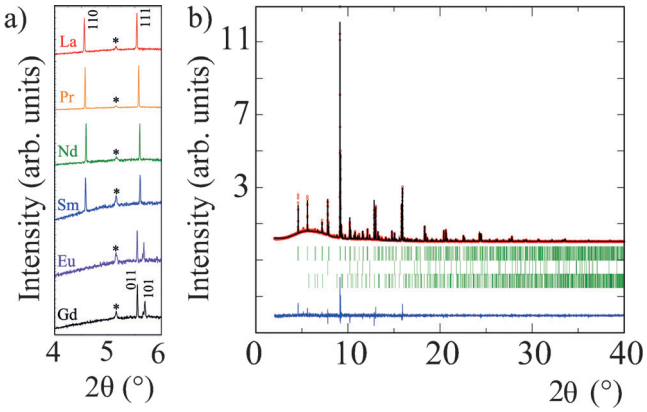

Figure 1. a) Low-angle powder synchrotron X-ray diffraction (SXRD) data ($\lambda = 0.4421$ Å) for $MnRMnSbO_6$ samples. The (110) peak (indexed on a 2×2×2 perovskite cell) characterizes the columnar order of A cations for the R = La, Pr, Nd, and Sm $P4_2/n$ double double perovskites. The (111) peak reveals rock salt type B-cation order, although this is split into (011) and (101) due to monoclinic distortion for R = Eu and Gd $P2_1/n$ double perovskites. The additional peak (*) is due to parasitic scatter from the diffractometer. b) Rietveld fit to synchrotron X-ray data for $MnNdMnSbO_6$; markers show additional contributions from TiO_2 (parasitic scatter from the detector) and less than 3%wt. of a $NdMnO_3$ secondary phase.

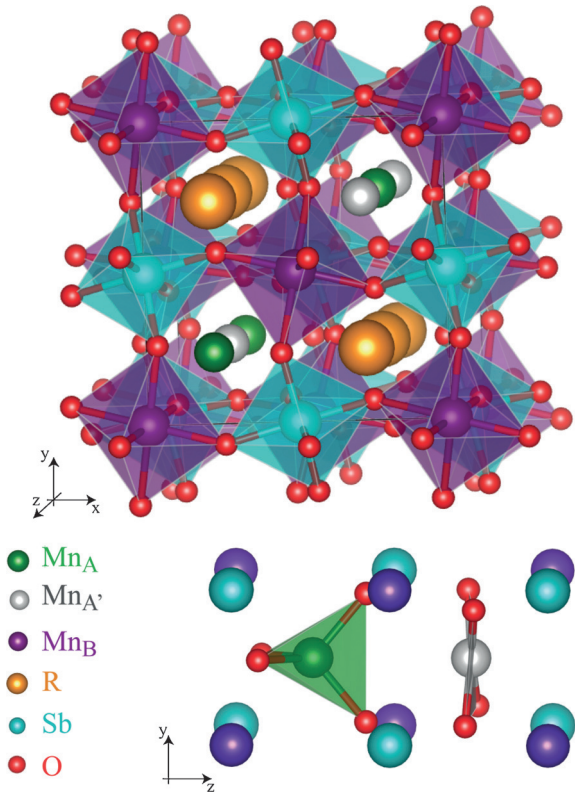

Figure 2. Double double perovskite structure of $MnRMnSbO_6$ oxides (R = La, Pr, Nd, and Sm).[18] B-site MnO_6 and SbO_6 octahedra have a rock salt type order whereas A-site Mn and R are ordered in columns parallel to the unique z-axis. Mn A sites are further split into Mn_A and $Mn_{A'}$ environments with tetrahedral and square-planar coordination modes as shown below.

ray analysis of a $MnNdMnSbO_6$ single crystal.[18] The refinement results are given in Table 1 and the structure is shown in Figure 2. This tetragonal arrangement has a 2×2×2 perovskite supercell with $P4_2/n$ symmetry and a very high degree of cation order, although a small excess of Mn was found at the Nd and Sb sites. Bond valence sum (BVS) calculations using the bond distances shown in Table 1 confirm the $Mn^{2+}Nd^{3+}Mn^{2+}Sb^{5+}O_6$ charge distribution with columnar Mn^{2+}/Nd^{3+} order at A sites and rock salt Mn^{2+}/Sb^{5+} cation order at the perovskite B sites.

Table 1: Refinement results[18] for $MnNdMnSbO_6$ at 120 K from single-crystal structure analysis with $Mo_{K\alpha}$ radiation.[a]

	x	y	z	$U_{eq.}$ [Å^2]	BVS
Mn_A	1/2	1/2	0	0.005	1.9
$Mn_{A'}$	0	0	0	0.019	1.8
Nd[b]	1/2	0	0.2674(4)	0.006	2.8
Mn_B	3/4	1/4	1/4	0.006	2.2
Sb[b]	1/4	1/4	1/4	0.003	5.4
O1	0.3194(3)	0.0097(3)	0.2820(3)	0.007	
O2	0.4855(3)	0.2920(3)	0.1655(4)	0.009	
O3	0.3192(4)	0.3004(4)	0.4855(3)	0.009	

Bond	Length [Å]	Bond	Length [Å]
Mn_A–O3 (×4)	2.110(3)	Mn_B–O1 (×2)	2.118(3)
$Mn_{A'}$–O2 (×4)	2.091(3)	Mn_B–O2 (×2)	2.199(3)
Nd–O1 (×2)	2.465(3)	Mn_B–O3 (×2)	2.196(3)
Nd–O1 (×2)	2.397(3)	Sb–O1(×2)	1.973(3)
Nd–O2 (×2)	2.536(3)	Sb–O2 (×2)	1.987(3)
Nd–O3 (×2)	2.762(3)	Sb–O3 (×2)	1.979(3)
Nd–O3(×2)	2.946(3)		

[a] Atomic coordinates (*x*, *y*, *z*), equivalent thermal factors ($U_{eq.}$), and bond valence sum calculations (BVS) are given (upper portion of the table). Bond lengths (< 3 Å) are given in the lower section. [b] Nd site has 6.3(6)% Mn occupancy and Sb has 7.6(6)% Mn. All other sites are occupied only by the element shown.

A-type Mn^{2+} cations in $MnNdMnSbO_6$ have two alternating inequivalent sites within their column and cooperative oxide displacements result in almost regular tetrahedral and square-planar environments as shown at the bottom of Figure 2. In contrast, Nd cations are 10-coordinate. The $MnNdMnSbO_6$ structure is thus notable for having five different cation sites, with three occupied by Mn^{2+} in tetrahedral, square-planar, and octahedral environments. Bond angles are 102.5(1) and 113.1(1)° in the Mn_AO_4 tetrahedron, and 90.2(1) and 173.8(1)° in the $Mn_{A'}O_4$ square plane. Mn_BO_6 octahedra have a slight tetragonal compression whereas SbO_6 octahedra are very regular, but the B-site octahedra are highly tilted as shown in Figure 2. Similar large internal distortions are found when transition-metal cations occupy 4-coordinate A sites in other perovskites. A-site Mn^{2+} has an approximate tetrahedral coordination in the double perovskites Mn_2FeSbO_6, Mn_2FeReO_6, and Mn_2MnReO_6. The large family of A-cation ordered $AA'_3B_4O_{12}$ perovskites have square-planar A′ sites that may be occupied by Mn^{2+} ions, for example in $(La_{0.5}Na_{0.5})Mn_3Ti_4O_{12}$.[12] Rock salt B-cation order can also occur in this family, leading to $AA'_3B_2B'_2O_{12}$ double

double perovskites, including the spintronic material $CaCu_3Fe_2Re_2O_{12}$.[13]

Structures of the $MnRMnSbO_6$ materials were further characterized using powder X-ray and neutron data and electron microscopy, and detailed results are reported in the Supporting Information. Electron diffraction confirms the $P4_2/n$ symmetry and no further superstructure was detected. The [110] lattice image of $MnPrMnSbO_6$ in Figure 3 shows microscopic order of both A- and B-site cations in the new double double perovskite arrangement.

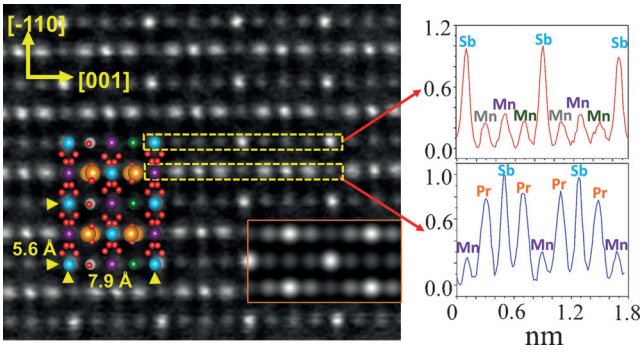

Figure 3. High-resolution [110] electron microscopy image of $MnPrMnSbO_6$ (left) with the cation-ordered double double perovskite model from Figure 2 (inset). The scanned intensities (right) from the dashed box sections in the main image show the Sb-$Mn_{A/A'}$-Mn_B-$Mn_{A/A'}$-Sb and Mn_B-Pr-Sb-Pr-Mn_B repeat sequences parallel to [001], where electron-rich Pr and Sb columns appear as bright spots and Mn are faint. These scans and the image simulation (lower right, orange box) confirm the high degree of cation order at perovskite A and B sites.

Although the $P4_2/n$ perovskite supercell has been reported previously, for example, in double perovskites $(SrNd)MRuO_6$ (M = Mg, Zn, Ni, Co),[14] these materials do not have cation order at the A sites. The $MnNdMnSbO_6$ structure discovered here is thus notable as a new $AA'BB'O_6$ double double perovskite type and the first to have magnetic transition-metal cations at A sites. The structure combines (110) columnar A-cation and (111) rock salt B-cation orders. Columnar A-cation order is rare but has been reported previously in $CaMTi_2O_6$ (M = Fe, Mn) double perovskites,[15,16] and columnar A-site charge order also occurs in the ambient-pressure structure of $BiNiO_3$ ($Bi^{3+}Bi^{5+}Ni_2O_6$).[17] 1:1 columnar order thus appears to be favored for accommodating A cations of very different coordination number, with 4-coordinate sites for transition-metal cations such as Mn^{2+} and 10-coordination for larger electropositive cations such as Ca^{2+} or the early rare earth metals. Combining this with usual size and charge differences for B-cation rock salt order stabilizes the $MnNdMnSbO_6$ double double perovskite type. In contrast, the $NaLaMgWO_6$ type is found for less extreme cation size mismatch at the A sites, but with strong off-center B-cation displacements (second-order Jahn–Teller effect) for highly charged d^0 cations such as W^{6+}.

Low-temperature magnetic susceptibility data for the $MnRMnSbO_6$ double double perovskites are shown in Figure 4, and the Supporting Information contains further magnetic results for all samples. These materials are paramagnetic at high temperatures and a Curie–Weiss fit to 150–300 K susceptibility for $MnNdMnSbO_6$ gives an effective

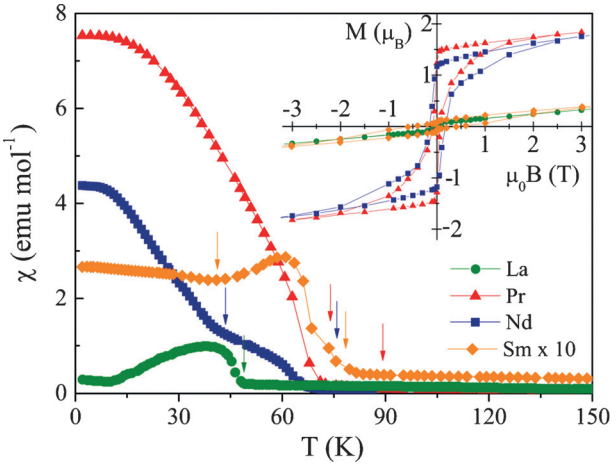

Figure 4. Magnetic susceptibilities of $MnRMnSbO_6$ double double perovskites in a 0.1 T field with arrows showing Curie and spin reorientation transitions. Susceptibilities for the Sm-containing structure are multiplied by 10 for visibility. Inset: Magnetization hysteresis loops at 2 K.

paramagnetic moment of $\mu_{exp} = 8.9\ \mu_B$ per formula unit, in good agreement with the theoretical value of 9.14 μ_B from $S = 5/2\ Mn^{2+}$ and $^4I_{9/2}\ Nd^{3+}$ ground-state contributions. A negative Weiss temperature ($\theta = -80$ K) shows that antiferromagnetic interactions are dominant. All of the double double $MnRMnSbO_6$ perovskites show Curie transitions (T_C) between 50 and 90 K (T_C values and other parameters are in the Supporting Information). The phases with magnetic R^{3+} cations also show a second magnetic transition as indicated on Figure 4. Magnetic hysteresis loops at 2 K show that the R = La and Sm materials have small saturated magnetizations of about 0.1 μ_B but structures with R = Pr and Nd have more substantial values of 1.5 and 1.2 μ_B.

Powder neutron diffraction data were used to explore the low-temperature magnetic order in $MnNdMnSbO_6$. On cooling below $T_C = 76$ K, magnetic peaks such as (200) appear (Figure 5a). These are indexed by propagation vector (0 0 0) and the 60 K data are fitted well by a simple antiferromagnetic model in which Mn A-site spins are antiparallel to B-site spins, with all moments in the z direction (Figure 5c). This arrangement and the negative Weiss temperature are consistent with antiferromagnetic $Mn_{A/A'}$-O-Mn_B interactions being dominant. On cooling below the second 42 K magnetic transition indicated by the magnetization anomaly in Figure 4, (00l) magnetic peaks such as (002) grow in intensity while (200) decreases. This result reveals a spin reorientation transition driven by order of the Nd moments in the xy-plane, probably driven by single-ion anisotropy of the Nd ion. The Mn moments rotate from being parallel to the z axis above

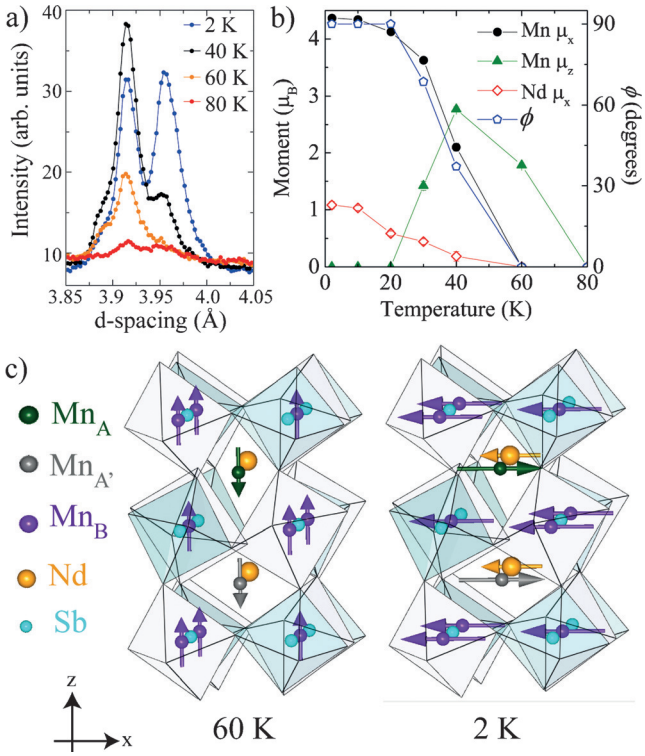

Figure 5. a) Magnetic contributions to the (200) and (002) neutron diffraction peaks at $d = 3.91$ and 3.95 Å, respectively, for $MnNdMnSbO_6$. The onset of antiferromagnetic Mn spin order is marked by the appearance of (200) intensity at 60 K, and changes between 40 and 2 K show the reorientation transition driven by Nd spin ordering. b) Temperature variations of the ordered *x* and *z* components of the Mn and Nd moments, and of the polar angle (ϕ) for Mn moments. $\mu_z = 0$ below 20 K where the reorientation transition is complete. c) Magnetic structures of $MnNdMnSbO_6$ at 60 and 2 K.

the 42 K transition to perpendicular below 20 K, as shown in Figure 5b. The 2 K magnetic structure has Mn^{2+} moments of 4.4 μ_B, close to the ideal value of 5 μ_B, but the ordered Nd^{3+} moment has a value of only 1.1 μ_B. This is consistent with the bulk magnetizations in Figure 4, as the A- and B-site Mn spins approximately cancel so the net magnetizations result from the ordered R^{3+} moments which are significant (about 1 μ_B) for Pr and Nd derivatives but zero or very small for La- and Sm-containing structures.

In conclusion, this study shows that using high pressure to stabilize Mn^{2+} at A sites can lead to the discovery of new cation ordered perovskite structure types. The new type of double double perovskite structure in the $MnRMnSbO_6$ (R = La, Pr, Nd, and Sm) family has a columnar order of A-site Mn^{2+} and R^{3+} cations whereas Mn^{2+} and Sb^{5+} have rock salt order on the B sites. Mn^{2+} cations are in tetrahedral and square-planar A-site environments and octahedral B sites. The $MnRMnSbO_6$ double double perovskites are ferrimagnetic at low temperatures with Curie transitions between 50 and 90 K and those with magnetic R^{3+} cations also show a second magnetic transition. Magnetic neutron data show that the direction of ferrimagnetic Mn spins in $MnNdMnSbO_6$ changes from parallel to [001] below $T_C = 76$ K to perpendicular below the reorientation transition at 42 K at which Nd moments also order. The tetragonal double double perovskite structure is stabilized by large R^{3+} cations and smaller rare earths lead to conventional monoclinic double perovskites $(MnR)MnSbO_6$ for R = Eu and Gd, where Mn^{2+} and R^{3+} are disordered over the A sites whereas Mn^{2+} and Sb^{5+} have rock salt order at the B sites. Thus, variation of the type and size of cation to control cation ordering and octahedral tilts under high-temperature and high-pressure conditions may lead to the discovery of other new ordered perovskites with novel structures and properties.

Acknowledgements

We acknowledge the EPSRC, the Royal Society, and STFC for support and provision of beam time at ISIS. MINECO and Comunidad de Madrid are also acknowledged for support through projects MAT2013-44964 and S-2013/MIT-1275. We thank Dr. P. Manuel and Dr. D. Khalyavin for assistance with neutron diffraction experiments on WISH. Synchrotron diffraction experiments were performed at ALBA beamline BL04-MSPD with the help of Dr. O. Vallcorba and Dr. C. Popescu. We thank the ICTS Centro Nacional de Microscopía Electrónica of U.C.M. for technical assistance.

Keywords: double perovskites · high-pressure chemistry · magnetic properties · perovskite phases · solid-state structures

How to cite: *Angew. Chem. Int. Ed.* **2016**, *55*, 9340–9344
Angew. Chem. **2016**, *128*, 9486–9490

[1] G. King, P. M. Woodward, *J. Mater. Chem.* **2010**, *20*, 5785.
[2] S. Vasala, M. Karppinen, *Prog. Solid State Chem.* **2015**, *43*, 1.
[3] S. García-Martín, E. Urones-Garrote, M. C. Knapp, G. King, P. Woodward, *J. Am. Chem. Soc.* **2008**, *130*, 15028.
[4] M. C. Knapp, P. M. Woodward, *J. Solid State Chem.* **2006**, *179*, 1076.
[5] M. Markkula, A. M. Arévalo-López, A. Kusmartseva, J. A. Rodgers, C. Ritter, H. Wu, J. P. Attfield, *Phys. Rev. B* **2011**, *84*, 094450.
[6] A. J. Dos santos-García, E. Solana-Madruga, C. Ritter, D. Ávila-Brande, O. Fabelo, R. Sáez-Puche, *Dalton Trans.* **2015**, *44*, 10665.
[7] E. Solana-Madruga, A. J. Dos santos-García, A. M. Arévalo-López, D. Ávila-Brande, C. Ritter, J. P. Attfield, R. Sáez-Puche, *Dalton Trans.* **2015**, *44*, 20441.
[8] A. J. Dos santos-García, C. Ritter, E. Solana-Madruga, R. Sáez-Puche, *J. Phys. Condens. Matter* **2013**, *25*, 206004.
[9] A. M. Arévalo-López, G. M. McNally, J. P. Attfield, *Angew. Chem. Int. Ed.* **2015**, *54*, 12074; *Angew. Chem.* **2015**, *127*, 12242.
[10] M.-R. Li, M. Retuerto, Z. Deng, P. W. Stephens, M. Croft, Q. Huang, H. Wu, X. Deng, G. Kotliar, J. Sanchez-Benitez, J. Hadermann, D. Walker, M. Greenblatt, *Angew. Chem. Int. Ed.* **2015**, *54*, 12069; *Angew. Chem.* **2015**, *127*, 12237.
[11] A. M. Arévalo-López, F. Stegemann, J. P. Attfield, *Chem. Commun.* **2016**, *52*, 5558.
[12] T. Tohyama, M. S. Senn, T. Saito, W.-T. Chen, C. C. Tang, J. P. Attfield, Y. Shimakawa, *Chem. Mater.* **2013**, *25*, 178.
[13] W. T. Chen, M. Mizumaki, H. Seki, M. S. Senn, T. Saito, D. Kan, J. P. Attfield, Y. Shimakawa, *Nat. Commun.* **2014**, *5*, 3909.
[14] E. Iturbe-Zabalo, J. M. Igartua, A. Faik, A. Larrañaga, M. Hoelzel, G. J. Cuello, *J. Solid State Chem.* **2013**, *198*, 24.
[15] K. Leinenweber, J. Parise, *J. Solid State Chem.* **1995**, *114*, 277.

[16] A. Aimi, D. Mori, K. Hiraki, T. Takahashi, Y. J. Shan, Y. Shirako, J. Zhou, Y. Inaguma, *Chem. Mater.* **2014**, *26*, 2601.
[17] M. Azuma, S. Carlsson, J. Rodgers, M. G. Tucker, M. Tsujimoto, S. Ishiwata, S. Isoda, Y. Shimakawa, M. Takano, J. P. Attfield, *J. Am. Chem. Soc.* **2007**, *129*, 14433.
[18] Crystal data for $MnNdMnSbO_6$: space group $P4_2/n$; $a = 7.8225(5)$ Å, $c = 7.9077(5)$ Å; $R_{obs} = 2.24\,\%$, $wR2 = 5.04\,\%$, GOF = 1.20. Further crystallographic data are in the Supporting Information and Open Data.

Received: April 11, 2016
Revised: May 10, 2016
Published online: June 17, 2016

